



**HAL**  
open science

## Discrete duality finite volume applied to soil erosion

Jalal Lakhili, Cédric Galusinski, Frédéric Golay

► **To cite this version:**

Jalal Lakhili, Cédric Galusinski, Frédéric Golay. Discrete duality finite volume applied to soil erosion. CFM 2015 - 22ème Congrès Français de Mécanique, Aug 2015, Lyon, France. hal-03444737

**HAL Id: hal-03444737**

**<https://hal.science/hal-03444737>**

Submitted on 23 Nov 2021

**HAL** is a multi-disciplinary open access archive for the deposit and dissemination of scientific research documents, whether they are published or not. The documents may come from teaching and research institutions in France or abroad, or from public or private research centers.

L'archive ouverte pluridisciplinaire **HAL**, est destinée au dépôt et à la diffusion de documents scientifiques de niveau recherche, publiés ou non, émanant des établissements d'enseignement et de recherche français ou étrangers, des laboratoires publics ou privés.

# Discrete Duality Finite Volume applied to soil erosion

J. LAKHLILI<sup>a</sup>, C. GALUSINSKI<sup>b</sup>, F. GOLAY<sup>c</sup>

a. IMATH - Université de Toulon, La Garde, France. email : lakhlili@univ-tln.fr

b. IMATH - Université de Toulon, La Garde, France. email : galusins@univ-tln.fr

c. IMATH - Université de Toulon, La Garde, France. email : golay@univ-tln.fr

## Résumé :

*L'objectif de cette étude est de simuler l'érosion d'un sol sous l'effet de l'écoulement d'un fluide. Suite aux travaux [1] et [2], des équations de conservation avec relation de sauts conduisent au modèle d'érosion. Une méthode de pénalisation est utilisée pour calculer les équations de Navier-Stokes autour d'un obstacle, avec une méthode aux domaines fictifs pour s'affranchir d'un maillage dépendant de la géométrie. L'interface eau/sol est décrite par une fonction Level Set couplée à une loi d'érosion à seuil. Nous proposons un schéma DDFV (Discrete Duality Finite Volume), autorisant des raffinements locaux sur maillages non-conformes et non-structurés. La pertinence du modèle à prédire l'érosion de surface du sol est confirmée par la présentation de plusieurs résultats de simulation 2D et 3D.*

## Abstract :

*This study focuses on the numerical modeling of the surface erosion occurring at a fluid/soil interface undergoing a flow process. Following a previous work [1] and [2], the balance equations with jump relations are used to exhibit the erosion model. The difficulty is then to compute accurately the erosion velocity of this free boundary problem. The ability of the model to predict the interfacial erosion of soils is confirmed by presenting several 2D and 3D simulations.*

**Mots clefs : interfacial erosion, incompressible flow, Navier-Stokes, fictitious domains, discrete duality finite volume, adaptive mesh refinement, Level Set.**

## 1 Introduction

Erosion phenomena is one of the main causes of the failure of hydraulic works such as dams, dykes and levees. In this context, the numerical modeling of the piping erosion of soil is a challenging problem [1], [2]. The model validated in [3] considers the erosion of a cohesive soil generated by a water flow tangential to the soil/water interface. The threshold erosion law is described by the shear stress of water at the soil/water interface.

A penalization procedure is used to compute Navier-Stokes equations around obstacles, with a fictitious domain method, in order to avoid body-fitted unstructured meshes. The water/soil interface evolution is described with a Level Set function coupled to a threshold erosion law. We are concerned with an accurate computation of the shear stress at the soil/water interface and we present test case to validate our approach. As the accuracy of the model depends strongly on the mesh discretization around the soil/water interface, adaptive mesh refinement is used, contrary to [3] where the mesh is a staggered cartesian grid. This obliges to use an adapted space discretization to Navier-Stokes equations, Discrete Duality Finite Volume scheme (DDFV) are chosen.

## 2 Physical model

The erosion model is described in [3], [4] and [5]. We consider an impervious soil under a diluted flow. With these assumptions, the solid/water interface can be considered as a sharp interface. As proved in [3], the time scales of the flow and of the erosion process are so different that the flow is described by the stationary Navier-Stokes equations at moderate Reynolds numbers. The velocity in the soil  $\mathbf{u}_s$  is assumed to vanish and the soil/water interface  $\Gamma$  is driven by the threshold law of erosion.

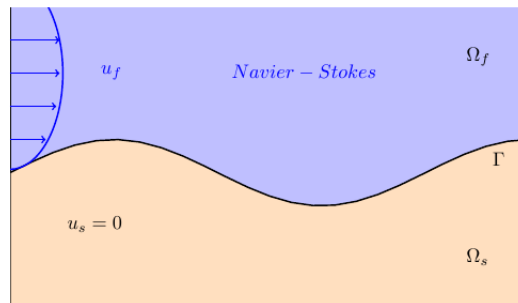


Figure 1: Erosion model

### 2.1 Governing equations

Let's denote  $\Omega_f$  the fluid domain and  $\Omega_s$  the soil domain. The fictitious domain approach, introduced by Angot in [10] and used by Golay *et al.* in [3], allows to describe

the behavior of the two subdomains with a Navier-Stokes system defined on the whole domain  $\Omega = \Omega_f \cup \Omega_s$ :

$$\begin{cases} \rho(\partial_t \mathbf{u} - \mathbf{u} \wedge \text{rot}(\mathbf{u})) - \mu \Delta \mathbf{u} + \nabla p = \rho \mathbf{g} - \frac{\mu H}{K_s} (\mathbf{u} - \mathbf{u}_s), \\ \text{div}(\mathbf{u}) = 0, \\ (+ \text{B.C.}) \end{cases} \quad (1)$$

Where  $\mathbf{u}$  is the flow velocity,  $p$  is the pressure,  $\rho$  is the water density,  $\mu$  is the dynamic viscosity and  $\rho \mathbf{g}$  represents the gravity force. The penalization coefficient  $K_s$  can be interpreted as a low permeability and  $H$  is the characteristic function of the soil domain, which is unity within  $\Omega_s$  and zero elsewhere. The boundary conditions (B.C.) closing the system are determined according to the considered problem.

## 2.2 Erosion law

The erosion law is an experimental law, validated by S. Bonelli [1] and R. Fell [2], which describes the interface behaviour. This threshold law links the eroded mass and the shear stress of the flow:

$$\dot{m}_{er} = \begin{cases} K_{er}(\tau - \tau_c) & \text{if } \tau > \tau_c, \\ 0 & \text{otherwise,} \end{cases} \quad (2)$$

where  $\tau_c$  is the critical shear stress and  $K_{er}$  is the kinetic coefficient of erosion. The tangential shear stress is given by :  $|\tau| = \sqrt{(\mathbf{T} \cdot \mathbf{n})^2 - (\mathbf{n} \cdot \mathbf{T} \cdot \mathbf{n})^2}$ , where  $\mathbf{T} = -p\mathbf{I}_d + 2\mu\mathbf{D}(\mathbf{u})$  denotes the stress tensor,  $\mathbf{D}(\mathbf{u})$  the symmetric velocity gradient and  $\mathbf{n}$  the exterior normal unit vector of the interface  $\Gamma$ . Based on the above assumption, the interface velocity is defined as follows ( $\rho_s$  is the soil density):

$$\mathbf{v}_\Gamma = \frac{\dot{m}_{er}}{\rho_s} \mathbf{n}. \quad (3)$$

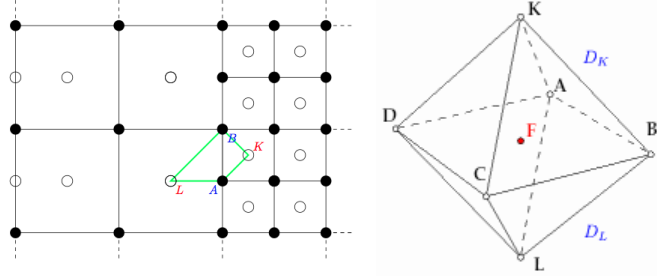
## 3 Numerical modeling

### 3.1 DDFV scheme

The DDFV methods can be seen as a generalization for unstructured mesh of the Marker and Cell (MAC) methods for Cartesian grids. A 2D and 3D DDFV scheme was proposed and tested in several studies. The one we implement is based on the versions developed by B. Andreinov in [6], Y. Coudiere and F. Hubert in [7], [8].

- **Meshes and notations:**

The DDFV mesh is defined as a couple of dual meshes  $\mathcal{M} = (\mathcal{T}, \mathcal{D})$ , where  $\mathcal{T}$  is a set containing cells of center  $K$  and vertices  $A$  and  $\mathcal{D}$  is a diamond mesh, related to the faces  $F$ .

Figure 2: 2D DDFV mesh example and 3D diamond ( $D_F = D_K \cup D_L$ )

The velocity  $\mathbf{u}^{\mathcal{T}}$ , defined on  $\mathcal{T}$ , the pressure  $p^{\mathcal{D}}$ , defined on  $\mathcal{D}$ , are respectively element of  $(\mathbb{R}^3)^{\mathcal{T}}$  and  $\mathbb{R}^{\mathcal{D}}$ . To each element  $X$  (cell center  $K$ , cell vertex  $A$ ), a control volume is associated and denoted by  $|X|$ . For example, in figure 2,  $|D_F|$  represent the volume of the diamond  $D_F = (K, L, A, B, C, D)$ . The interface between two control volumes  $(X, Y)$  is carried by a normal vector  $\mathbf{N}_{XY}$ . The interfaces vectors are defined by:  $\mathbf{N}_{KL} = \frac{1}{2}\overrightarrow{AC} \wedge \overrightarrow{BD}$ ,  $\mathbf{N}_{AC} = \frac{1}{2}\overrightarrow{KL} \wedge \overrightarrow{BD}$ ,  $\mathbf{N}_{BD} = \frac{1}{2}\overrightarrow{AC} \wedge \overrightarrow{KL}$ .

• **Discrete operators (3D) :**

- The discrete gradient is a consistent approximation of the gradient operator of each component  $u^{\mathcal{T}} = (u_K, u_L, u_A, u_B, u_C, u_D)$  of  $\mathbf{u}^{\mathcal{T}} \in (\mathbb{R}^3)^{\mathcal{T}}$  and is defined by:

$$\nabla^{\mathcal{D}} u^{\mathcal{T}} = \frac{1}{3|D_F|} ((u_L - u_K)\mathbf{N}_{KL} + (u_C - u_A)\mathbf{N}_{AC} + (u_D - u_B)\mathbf{N}_{BD}).$$

- The discrete divergence is a consistent finite volume approximation of the divergence operator applied to the discrete tensor field  $\mathbf{q}^{\mathcal{D}} \in (\mathbb{R}^3)^{\mathcal{D}}$  and is defined by:

$$\operatorname{div}^{\mathcal{T}}(\mathbf{q}^{\mathcal{D}}) = (\operatorname{div}_K(\mathbf{q}^{\mathcal{D}}), \operatorname{div}_A(\mathbf{q}^{\mathcal{D}}))_{K, A \in \mathcal{T}},$$

where:

$$\operatorname{div}_K(\mathbf{q}^{\mathcal{D}}) = \frac{1}{|K|} \sum_{D \in \mathcal{D}} \mathbf{q}^{\mathcal{D}} \cdot \mathbf{N}_{KL} \text{ and } \operatorname{div}_A(\mathbf{q}^{\mathcal{D}}) = \frac{1}{|A|} \sum_{D \in \mathcal{D}} \mathbf{q}^{\mathcal{D}} \cdot \mathbf{N}_{AC}$$

• **Global operators:**

Thereafter, using the discrete gradient  $\nabla^{\mathcal{D}}$  and discrete divergence  $\operatorname{div}^{\mathcal{T}}$  we are able to build several operators:

$$\begin{aligned} \operatorname{div}^{\mathcal{D}} \mathbf{u}^{\mathcal{T}} &= \operatorname{tr}(\nabla^{\mathcal{D}} \mathbf{u}^{\mathcal{T}}) & \nabla^{\mathcal{T}} q^{\mathcal{D}} &= \operatorname{div}^{\mathcal{T}}(q^{\mathcal{D}} \mathbf{I}_d) \\ \operatorname{rot}^{\mathcal{T}} \mathbf{q}^{\mathcal{D}} &= \nabla^{\mathcal{T}} \wedge \mathbf{q}^{\mathcal{D}} & \Delta^{\mathcal{T}} \mathbf{u}^{\mathcal{T}} &= \operatorname{div}^{\mathcal{T}} \nabla^{\mathcal{D}} \mathbf{u}^{\mathcal{T}} \end{aligned}$$



### 3.3 Level Set method

The Level Set function  $\phi$  [11], is defined as the signed distance to the soil/water interface. The soil/water interface  $\Gamma$  is represented by the zero level set of  $\phi$ . We consider that in the soil  $\phi > 0$  and in the fluid  $\phi < 0$ .

The displacement of the interface is driven by a transport equation:

$$\begin{cases} \partial_t \phi + \mathbf{v}_\Gamma^{ext} \cdot \nabla \phi & = 0 \\ \phi(x, t = 0) & = \phi_0, \end{cases} \quad (6)$$

where  $\mathbf{v}_\Gamma^{ext}$  is an extension on the whole domain of the interface celerity  $\mathbf{v}_\Gamma$  given previously in (3) and  $\phi_0$  is the initial position of the Level Set function.

### 3.4 The shear stress estimation

To avoid remeshing in moving interface problems, we are concerned with non-body-fitted mesh. Coupled with a penalty method to take into account a free velocity in the soil, an inaccurate shear stress is computed at the interface  $\Gamma$ . Indeed, the shear stress depends on the velocity gradient. As the penalized velocity in the soil vanishes, an inconsistent value of velocity gradient on the boundary appears. This problematic is already met in Stefan problem [12] and solved for example with Immersed Interface Method (IIM) of LeVeque and Li [13], instead of penalty method. With IIM, continuity properties at the discontinuity interface are satisfied thanks to Taylor expansions of the solution on each side of the interface.

Keeping in mind penalty methods, we propose to improve the shear stress computation according to two alternatives:

- **Alternative 1:** Considering that gradient inconsistency is located in a neighborhood of the interface, the inaccurate shear stress is limited about four cells of size  $h$  near  $\Gamma$ . It is then pertinent to compute the shear stress where the Level Set  $\phi$  is close to  $-4h$ , corrected with the linear extrapolation in order to evaluate it on  $\Gamma$ :

$$\tau^* = \tau - \phi \nabla \tau \cdot \frac{\nabla \phi}{|\nabla \phi|}. \quad (7)$$

- **Alternative 2:** We build a smooth extension of the velocity inside the soil in order to eliminate the inaccurate boundary layer. A velocity field being given in the fluid domain, a  $C^1$ -extension of this velocity is defined in the soil by constructing the symmetric velocity with respect to the soil interface velocity.

First, we compute the velocity using penalization in the soil domain with free velocity. Secondly, we use the smooth extension above as penalized velocity in the soil. We iterate this process until convergence. This is a variant of what is proposed in [14].

A test is carried out on Taylor-Couette flow [2]. We consider the radial flow between two cylinders of radius  $r_1 = 0.2cm$  and  $r_2 = 0.4cm$ . The first interface  $r_1$  is an erodible one and the second one  $r_2$  is not. On figure 3, we represented the shear stress as a function of the radius for all diamonds of the three dimensional mesh. If we focus on the shear stress computed near the erodible interface, represented by the red line, we observe in the first case (3a) with a rigid penalization, that magnitude of the shear stress oscillates strongly. With the 1<sup>st</sup> alternative the error measured around  $\phi = -4h$  achieves 10% and with 2<sup>nd</sup> alternative the error measured around  $\phi = 0$  achieves 5%.

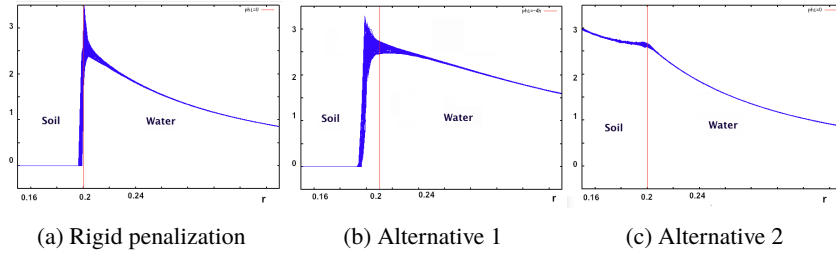


Figure 3: Rotating cylinder test - shear stress  $\tau(r)$  computed in several cases

The interface velocity is computed from  $\mathbf{v}_\Gamma = \frac{K_{er}}{\rho_s}(\tau - \tau_c)$  and extended on the whole domain thanks to the following transport equation propagating the information from the region  $\phi = \delta h$ :

$$\begin{cases} \partial_t \mathbf{v}_\Gamma^{ext} + \text{sgn}_h(\phi + \delta h) \frac{\nabla \phi}{|\nabla \phi|} \cdot \nabla \mathbf{v}_\Gamma^{ext} & = 0, \\ \mathbf{v}_\Gamma^{ext}(x, t = 0) & = \mathbf{v}_\Gamma \end{cases} \quad (8)$$

where:  $\delta = -4$  in the first alternative and  $\delta = 0$  in the second one. The function  $\text{sgn}_h(x)$  coincide with the sign function where  $|x| > \frac{h}{2}$  and vanishes where  $|x| \leq \frac{h}{2}$ .

## 4 Validation

The following simulations are carried out with the same erosion's parameters,  $\tau_c = 0Pa$  and  $\frac{K_{er}}{\rho_s} = 10^{-7}ms^{-1}Pa^{-1}$ , this choice of paramete will lead to a slow erosion velocity compared to the flow velocity in the studied examples.

### 4.1 Erosion of a soil ball

We consider the erosion of a fixed ball of soil (diameter  $0.2cm$ ) in a channel (section  $1cm \times 1cm$  and length  $2cm$ ). We impose a pressure gradient  $|\nabla p| = 1Pa/cm$  from the left to the right and a wall condition on the boundary except on the left and right (inflow and outflow) where a Neumann condition is imposed. The velocity is then of order  $1cm/s$ . The figure 4 shows the flow and an AMR mesh with a thin refinement around the ball.

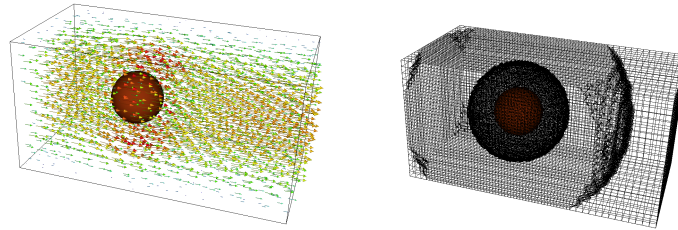


Figure 4: Flow around the ball and AMR mesh

The erosion of the ball is symmetric between inflow and outflow for Stokes flow, but for Navier-Stokes flow ( $Re = 100$ ), inertia makes the shear stress stronger on the upstream part of the ball. As expected and shown on figure 5, the shear stress is the strongest in region close the lateral walls where the flow is increased for the Stokes flow. The symmetry of the erosion is lost for Navier-Stokes flow.

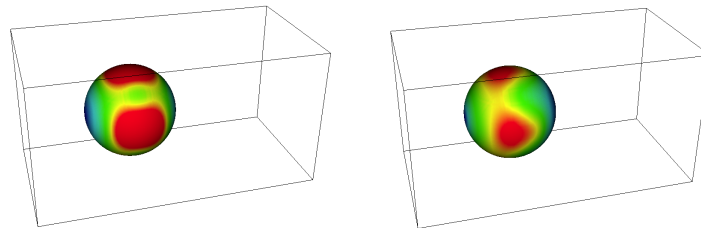


Figure 5: Shear stress on the ball for Stokes and Navier-Stokes flows

In figure 6 we show the evolution of the eroding ball on the central cut. As expected, during the erosion we observe that the ball shrinks by taking a symmetric oval shape under the Stokes flow, but, an asymmetric shape with strong erosion at inflow for Navier-Stokes flow.

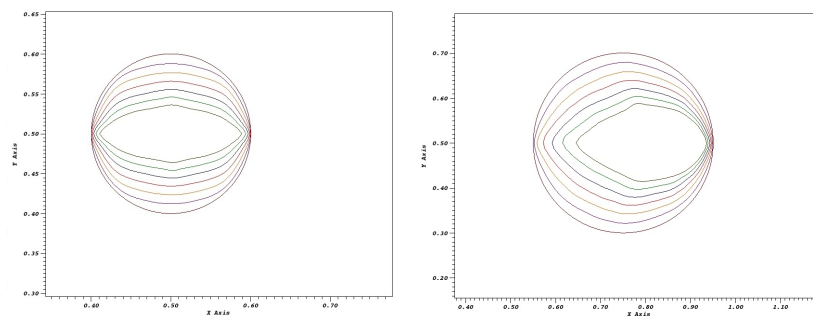


Figure 6: Erosion of the ball for Stokes and Navier-Stokes flows with alternative 1

## 4.2 Erosion of a soil cylinder

Now, we consider the erosion of a fixed cylinder (diameter  $0.2\text{cm}$ ) into a channel (section  $1\text{cm} \times 1\text{cm}$  and length  $2\text{cm}$ ). This two dimensional test case is chosen in order to estimate the erosion accuracy induced by alternative 2. We observe, on figure 7, a strong decrease of the shear stress from the interface through the flow. Even with a fine grid the shear stress variation is very important (50% on four cells). The alternative 2 is then more pertinent for this test case.

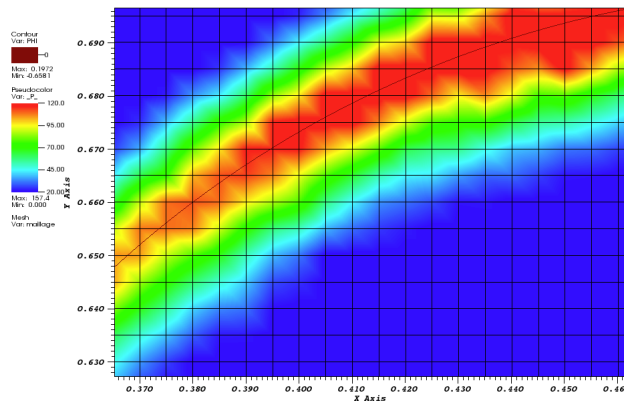


Figure 7: Zoom of shear stress around the interface

The complete process of erosion is introduced on figure 8 and shows a lower erosion on Stokes flow (inertia neglected) than for Navier-Stokes ( $Re = 100$ ). As a matter of fact, each curve corresponds to the soil/water interface at the same time. Then, for identical erosion law and flow rate, inertia enforces asymmetries in eroded shapes and eroded masses.

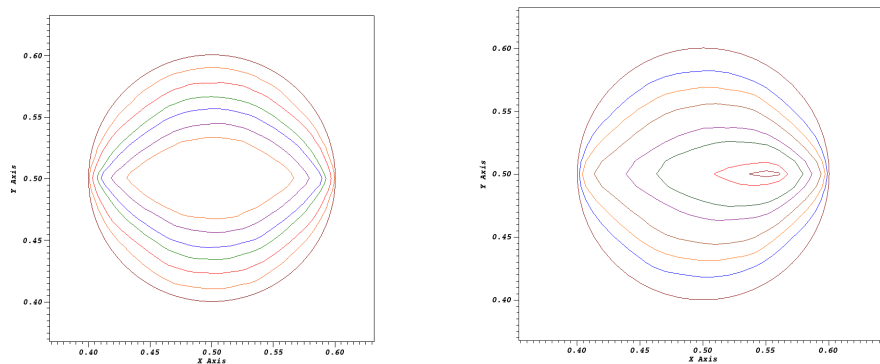


Figure 8: Erosion of soil cylinder for Stokes and Navier-Stokes flows

## Conclusion

We considered an erosion process of a cohesive soil subject to a water flow. The model is described as a free boundary problem for the soil/water interface driven by an erosion law. This law depends on the shear stress of a Navier-Stokes flow at the interface. The Navier-Stokes equations are approached with a DDFV scheme on AMR grids which do not fit to the moving interface. We then propose two alternatives to take into account, accurately, the erosion velocity. Finally, three test cases are introduced:

- the rotating cylinder test validates the two alternatives,
- the soil ball erosion test simulates a really 3D configuration,
- the soil cylinder erosion test exhibits strong shear stress variation.

Outgoing works will focus on a parametric study with respect to different Reynolds numbers and different kinetic coefficients of erosion. The results will then be compared to laboratory experiments. Finally, the aim is to couple water/soil erosion to air/water flows.

## References

- [1] S. Bonelli, O. Brivois: The scaling law in the hole erosion test with a constant pressure drop *Int. J. Numer. Anal. Meth. Geomech.*, 32, pp. 1573–1595, 2008.
- [2] C. Wan, R. Fell: Laboratory Tests on the Rate of Piping Erosion of Soils in Embankment Dams. *Journal of Geotechnical Testing Journal*, pp. 27–3, 2004.
- [3] F. Golay, D. Lachouette, S. Bonelli, P. Seppecher: Numerical modelling of interfacial soil erosion with viscous incompressible flows. *Comp. Meth. In App. Mech. And Eng.*, 200 (1-4), pp. 383-391, 2011.
- [4] S. Bonelli, F. Golay, D. Lachouette, F. Mercier: Erosion of geomaterials. *Chapter 6, ISTE, Wiley*, ISBN 9781848213517, 2012.
- [5] F. Golay, D. Lachouette, S. Bonelli, P. Seppecher: Interfacial erosion: a three-dimensional numerical model. *C.R. Mécanique*, 338 (6), pp. 333–337, 2010.
- [6] B. Andreianov, M. Bendahmane, F. Hubert, S. Krell: On 3D DDFV Discretization of gradient and divergence operators. I. Meshing, operators and discrete duality. *IMA J. Numer. Analysis*, 32 (4), pp. 1574–1603, 2012.

- 
- [7] Y.Coudiere, F Hubert: A 3D Discrete Duality Finite Volume method for nonlinear elliptic equations. *SIAM Journal on Scientific Computing*, 33 (4), pp. 1739–1764, 2011.
- [8] Y. Coudiere, C. Pierre: A 2D 3D Discrete Duality Finite Volume Scheme. Application to ECG simulation. *International Journal on Finite Volumes*, 6, 2009.
- [9] J.L. Guermond, P. Mineev, J. Shen: An overview of projection methods for incompressible flows. *Comput. Methods Appl. Mech. Engrg.*, 195 (44-47), pp. 6011–6045, 2006.
- [10] P. Angot, C.-H.Bruneau, P.Fabrie: A penalization method to take into account obstacles in incompressible viscous flowss. *Numer. Math.*, 81, pp. 497–520, 1999.
- [11] S. Osher, N. Paragios: Geometric Level Set Methods in Imaging, Vision, and Graphics. *Springer-Verlag New York, Inc.*, pp. 6140–6164, 2003.
- [12] F. Gibou, R.P. Fedkiw: A fourth order accurate discretization for the Laplace and heat equations on arbitrary domains, with applications to the Stefan problem. *J. Comput. Phys.*, vol. 202, pp 577–601, 2005.
- [13] R. J. LeVeque, L.Z. Li: The immersed Interface method for elliptic equations with discontinuous coefficients and singular sources. *SIAM J. Numer. Anal.*, 31, pp. 1019–1044, 1994.
- [14] F. Chantalat, C.H. Bruneau, C. Galusinski, A. Iollo: Level-set, penalization and Cartesian meshes: a paradigm for inverse problems and optimal design. *J. Comput. Phys.*, 17, pp. 6291–6315, 2009.